

Production of Macroporous Resins for Heavy-Metal Removal. I. Nonfunctionalized Polymers

Jesús Ortiz-Palacios,¹ Judith Cardoso,¹ Octavio Manero²

¹Departamento de Física, División De Ciencias Básicas E Ingeniería, Universidad Autónoma Metropolitana-Iztapalapa, Apartado Postal 55-534, México, D.F. 09340, México

²Instituto de Investigaciones en Materiales, Universidad Nacional Autónoma de México, Apartado Postal 70-360, México, D.F. 04510, México

Received 4 January 2007; accepted 13 August 2007

DOI 10.1002/app.27243

Published online 5 November 2007 in Wiley InterScience (www.interscience.wiley.com).

ABSTRACT: The aim of this work was the synthesis of macroporous resins with large specific surface areas through the use of organic solvents (known as porogens or pore-forming agents) for applications in hexavalent chromium (Cr^{+6}) removal operations. The synthesis of these materials by suspension polymerization allowed the generation of macroporous structures. The comonomers 4-vinylpyridine and divinylbenzene were considered in different ratios. Poly(vinyl alcohol) was used as a suspension agent in a mixture of toluene and hexane. The materials produced were characterized with Fourier transform infrared spectroscopy, elemental analysis, thermogravimetry, nitrogen adsorption, and scanning electron microscopy. The macroporous resin with the largest surface area ($130 \text{ m}^2/\text{g}$) was thermally stable up to 300°C and had a structure that included spherical domains

with a mean diameter of $68 \mu\text{m}$, uniform porosity, and expected high sorption capability. The sorption properties of the resins were evaluated for applications in water-treatment operations to eliminate Cr^{+6} ions at a pH near 7. The advantages of these materials were their high removal capability, high selectivity, and fast adsorption kinetics at a pH 6.5. An aqueous solution of 4 ppm $\text{K}_2\text{Cr}_2\text{O}_7$ was used to quantify the Cr^{+6} content by ultraviolet-visible spectroscopy. A remarkable sorption level (94%) of chromate ions (Cr^{+6}) was obtained during a 15-h period for the resin with the highest pyridine group content. © 2007 Wiley Periodicals, Inc. *J Appl Polym Sci* 107: 2203–2210, 2008

Key words: adsorption; macroporous polymers; metal-polymer complexes; morphology; synthesis

INTRODUCTION

The increasing accumulation of chromium in the environment from industrial output has caused great concern. Chromium compounds are extensively used in electroplating, anodizing operations for surface finishing, corrosion control, and oxidation, and leather, glass, ceramic, photography, and tanning industries. Chromium has three main forms: chromium (Cr^0), trivalent chromium (Cr^{+3}), and hexavalent chromium (Cr^{+6}). Cr^0 is not found in nature in the native form, although it is believed that in this form it is not a risk for health. On the other hand, Cr^{+3} is an essential nutrient for living organisms and is 100-fold less toxic than Cr^{+6} . The latter has a significant impact on human health and other living organisms. Toxicity to humans includes lung cancer, liver, kidney, and gastric damage, and epidermal irritation. Various technologies have been developed recently for the removal of these chromate ions (existing in aqueous solutions as oxyanions such as $\text{Cr}_2\text{O}_7^{-2}$, $\text{HCr}_2\text{O}_7^{-1}$, HCrO_4^{-1} , and CrO_4^{-2}) from wastewater to

prevent pollution in municipal and industrial wastes.^{1–5}

Precipitation is the method usually considered for chromium ion removal in water-treatment operations.^{6,7} This requires a reduction of Cr^{+6} to Cr^{+3} , although large residue concentrations exceed the limits allowed in the wastes. To improve the removal capacity, solvent extraction with tertiary amines has been also considered.^{8,9} In this respect, alternative processes such as anionic interchange are useful for Cr^{+6} removal in alkaline or acidic solutions in the presence of high chloride, sulfate, bicarbonate, and nitrate ion concentrations.^{10,11} Recently, Gang et al.¹² modified a poly(vinyl pyridine)-coated silica gel used for Cr^{+6} removal under very fast kinetics to increase the surface area.

There are many types of adsorbents, including activated carbon.^{13–15} Auki et al.¹⁶ reported the use of activated carbon for Cr^{+6} removal (up to 98%) and recovery in electrochemical plants. A concentration of 200 mg/L at various pH levels was considered, which is higher than the 100 mg/L concentration previously reported. On the other hand, anionic interchange resins made from styrene and divinylbenzene (DVB) possess good chromium removal capacity at pH levels of 3–4. For larger pH levels,

Correspondence to: J. Cardoso (jcam@xanum.uam.mx).

the removal capacity decreases steeply.¹⁷ The same behavior has been observed with other adsorbents, such as biomaterials,^{18,19} chitosan,²⁰ sawdust,¹ polyacrylamide-grafted sawdust,² and polyacrylonitrile fibers,³ that have been studied for the adsorption of chromium in aqueous solutions. However, some of these adsorbents do not have high adsorption capacities or need long adsorption equilibrium times, whereas others may present difficulties for regeneration and reuse. One of the recent developments in the removal of heavy-metal ions from water and wastewater is the use of polymer beads as adsorbents. This is mainly attributed to the relatively large external specific surface areas, high adsorption kinetics, and low cost of these polymer beads.^{5,21}

Synthetic macroporous resins are widely used in water-treatment operations and organic-compound removal. They are characterized by a permanent porous structure even when they are dried, and they swell less than gel-type resins. In addition, they do not require a porosity-generated solvent that allows the rapid diffusion of particles to the solid inner core.²² The porous structures are usually formed during copolymerization of mixtures of two monomers and the porogen agent. As a result, the final product usually has a broad pore size distribution often ranging from micropores to macropores. The use of an organic solvent as a porogen or pore former and the resulting phase separation induced during polymerization are crucial factors in controlling the average pore diameter and corresponding internal surface area of the resin. As a general guide, solvent porogens with poor thermodynamic compatibility with the incipient polymer network cause early phase separation and microgel formation.²² This allows the microgel particles to fuse, aggregate, and become infilled during the ensuing polymerization (the morphological structure coarsens). Overall, this gives rise to the formation of pores with a large average diameter and resins with a rather low surface area [e.g., $<50 \text{ m}^2/\text{g}$; N_2 sorption, Brunauer–Emmett–Teller (BET)]. In contrast, solvent porogens with good thermodynamic compatibility with the polymer network cause phase separation at a late stage in the polymerization, and so the microgel particles, although still becoming fused, tend to retain more of their individuality (the morphological structure does not coarsen). As a result, the average pore diameter is much lower, and the surface area of such resins is larger ($50\text{--}750 \text{ m}^2/\text{g}$). Further details on morphology control in resins prepared by suspension polymerizations are available in the literature.^{22–25} In addition, the type or amount of the pore-forming agent or porogen is important in the resulting pore structure and morphology of the polymer.

It is well known that polymers based on vinyl pyridine (VP) can form polymer–metal complexes.²⁶

Gutanu et al.¹⁴ found that the 4-vinylpyridine (4VP)–DVB copolymer retains Fe^{+3} ions from nitrogen– Fe^{+3} complexes. Sugii et al.²⁷ also proposed that polymers containing pyridine groups could retain metal ions by two mechanisms: conventional ion exchange and complexation. Recently, Rivas et al.¹⁹ described the high selective binding of mercury ions by a poly(4-vinylpyridine) hydrochloride resin. The mercury retention occurs in an acidic solution through the ion-exchange process of chloride anions by tetrahedral $[\text{HgCl}_4]^{2-}$ anions.

Neagu et al.²⁸ produced anionic interchange resins, using 4VP and DVB functionalized with aliphatic groups such as methyl, ethyl, and butyl moieties. The Cr^{+6} removal capacity increased with decreasing aliphatic group size. Arslan et al.²⁹ described the sorption of Cr^{+6} from aqueous solutions, using the batch method with poly(4-vinylpyridine). At a pH of 3.0, the maximum adsorption performance was achieved at 86.7 mg/g with 500 mg/L Cr(VI) solutions. The process of adsorption of Cr(VI) was described by the Langmuir isotherm.

In this work, the synthesis of macroporous resins with specific surface areas produced by suspension polymerization with 4VP and DVB as comonomers and various proportions of porogens (e.g., toluene and hexane) is reported. The sorption properties of the resins are evaluated for applications in water-treatment operations to eliminate Cr^{+6} ions at pHs near 7. The advantages of these materials are their high removal capability, high selectivity, and fast adsorption kinetics at pH 6.5. Commercial strong-base anionic resins usually show high removal capability but low selectivity for some metallic ions. Instead, the polystyrene-based chelating resins present high selectivity to metals, although the interchange kinetics are slow because of the hydrophobic character of the polystyrene polymer chain and that of the chelating group.^{17,30} In addition, the chelating resins are high-cost materials and cannot eliminate metals in anionic form, such as chromium and arsenic. The use of VPs increases the hydrophilic character of the resin and the capacity for the physical adsorption of anions on the sorbent surface.

EXPERIMENTAL

Materials

4VP (monomer; Aldrich, Milwaukee, WI) was purified by vacuum distillation. DVB (crosslinking agent; Aldrich) was a 55% isomeric mixture. The purification of DVB included a 5% NaOH washing stage to eliminate the red color and a second stage with distilled water. Poly(vinyl alcohol) (PVA; Aldrich; 80–87% hydrolyzed) had a molecular weight of 8500–12,400. Toluene and hexane were used as porogen

TABLE I
Synthesis Conditions and Swelling Properties of the Materials

Copolymer	Monomer (%)		Porogen	rpm	Swelling (%)	BET area (m ² /g)
	4VP	DVB				
PM40	60	40	100% toluene	470	43.94 ± 0.03	129.74
PM20	80	20	100% toluene	470	249.55 ± 0.03	1.20
PM10	90	10	40%/60% toluene/hexane	200	7.67 ± 0.03	15.24

The organic/aqueous phase ratio was 1/1; 33% of the organic phase was composed of the monomer mixture, and 66% was composed of the porogen agent.

agents. 2,2-Azobisisobutyronitrile (Aldrich, Milwaukee, WI) was used as an initiator.

Suspension polymerization

The 4VP–DVB copolymer was obtained by suspension polymerization. A four-necked, 1-L reaction vessel equipped with a thermostat, a stirrer, a water condenser, and a nitrogen inlet was used. The continuous phase (deionized water and a 2 wt % PVA solution) was placed in a reactor vessel, under stirring, at 70°C. At this temperature, the organic phase (the two monomers, azobisisobutyronitrile, and the porogen agent) was added. The mixture was heated to 80°C for 24 h. The copolymers were then isolated for filtration. The particles were washed with a methanol–water mixture to eliminate the residual monomer and PVA. The mixture was washed several times until turbidity disappeared. The material was filtered and dried in a vacuum oven at 50°C for 24 h.

Characterization

The copolymers were characterized with Fourier transform infrared (FTIR) spectroscopy (Spectrum GX, PerkinElmer, Norwalk, CT), elemental analysis (PerkinElmer, Norwalk, CT), thermogravimetry (Pyris TGA, PerkinElmer, Norwalk, CT), nitrogen absorption with the BET isotherm (Autosorb-1 apparatus, Quantachrome, Boynton Beach, FL), and scanning electron microscopy (SEM; DSM 940, Zess, Vertrieb, Deutschland).

Chromium sorption

The batch equilibrium method was used to measure the sorption properties of the polymers. The chromium solution (100 mL, 4 ppm) and 0.5 g of resin were added to an Erlenmeyer beaker at the ambient temperature, with the pH set to 6.5. On the other hand, the Langmuir isotherm was obtained with different amounts of metal ions (4–500 ppm) at a constant temperature and at pH 6.5. The chromium concentration was measured by ultraviolet–visible spectroscopy with a PerkinElmer Lambda 40. The

calibration curve was obtained with standard solutions with concentrations of 1–4 ppm. From each solution, 5-mL samples were taken, and 12 drops of sulfuric acid (0.18M) were added. Subsequently, diphenyl carbazide was added and left to rest for 10 min until the typical pink-violet color developed. Absorbance measurements of each sample gave a value of 540 nm.³¹

The sorption capability of the copolymers was calculated with the following expression:

$$q = (C_0 - C) \times V/m$$

where q is the adsorbed ion amount (mg/g); C_0 and C are the initial and current concentrations in the liquid phase, respectively; V is the volume of the solution (L); and m is the amount of poly(4-vinylpyridine) (g).

Measurements of the swelling properties

The copolymers were dissolved in water at the ambient temperature to reach equilibrium conditions. After treatment, water in excess was removed via blotting between filter paper.

The swelling amount (Q) was calculated according to

$$Q = (W_s - W_d)/W_d$$

where W_s and W_d are the weights of the swollen and dried copolymers, respectively.

RESULTS AND DISCUSSION

In Table I, the reaction conditions and properties of the pyridine copolymers are shown. The BET areas of the resulting polymers prepared with various porogen and DVB contents are also displayed. As the DVB content changes, the measured specific surface area is modified. The PM40 resin shows the largest surface area (130 m²/g) and a swelling degree of 43.94. The highest swelling degree is that of PM20, but it shows a surface area of only 1.20 m²/g. In con-

TABLE II
Elemental Analysis of the Polymers

Copolymer	Elemental analysis (%)					
	C		H		N	
	Experimental	Theoretical	Experimental	Theoretical	Experimental	Theoretical
PM10	77.0 ± 0.7	77.7	7.4 ± 0.4	8.3	9.7 ± 0.9	11.2
PM20	81.5 ± 0.7	81.3	7.4 ± 0.4	8.5	8.0 ± 0.9	10.0
PM40	85.7 ± 0.7	81.9	8.1 ± 0.4	8.4	4.7 ± 0.9	6.7

trast, the PM10 resin has the lowest swelling degree and surface area but the highest concentration of pyridine groups. According to the current literature, for lower DVB contents, the specific surface areas decrease, whereas for larger DVB contents, the areas should increase. If a 100% crosslinking agent is present, an 800 m²/g surface area can be generated.²² Our results confirm this observation.

Elemental analysis

Elemental analysis data of the precursor resins corrected for the water content [from thermogravimetric analysis (TGA)] are shown in Table II. The theoretical values were obtained under the assumption of stoichiometric proportions, and it was possible to calculate the real pyridine content incorporated into the polymer. The last column in Table II displays the theoretical values versus the experimental data for pyridine incorporated into the polymer. Because the reactivity coefficients of 4VP and DVB are similar (0.55), both monomers have the same probability to be incorporated into the polymer matrix. However, the nitrogen content in the three polymers presents a 20% difference with the theoretical content, and this shows that 4VP does not fully incorporate into the polymer chain, as also reported by Neagu et al.²⁸ A possible explanation considers the presence of four major components: *m*-DVB and *p*-DVB, typically in a ratio of ~ 2:1, and *m*-ethyl styrene and *p*-ethyl styrene in a similar ratio. In commercial-grade DVB, the isomer content is ~ 50%. Within simple copolymerization kinetics, the reactivity ratios of styrene and *m*-DVB are almost equal (0.58).²² However, the ratios of styrene and *p*-DVB are different (0.28 and

1.2, respectively), and this leads to higher incorporation of *p*-DVB into the copolymer. If we assume a similar pattern in *m*-DVB–4VP, a larger amount of the *p*-DVB isomer may then be expected. A larger amount of DVB induces a wider difference in the incorporation of 4VP.

TGA

Table III shows thermogravimetric data for the polymers. The resins present high thermal stability that is a function of the crosslinking agent content. The materials are a little hygroscopic (<5% water). At elevated temperatures, the chelating polymers decompose in a single stage within the 273–420°C interval.

SEM results

Figure 1(A) shows micrographs of the precursor resins with 100% toluene as a porogen agent. The microporous resin PM40, containing 40% crosslink agent (DVB) and pure toluene as a porogen agent, shows the largest surface area (130 m²/g), with spherical domains and a uniform size of 68 μm. The porosity of the spherical domains reveals a high specific surface area with an expected increased sorption capability. With a low crosslinking content, gel-type resin formation requires the presence of a porogen at a concentration that does not cause precipitation of the growing polymer.²³ With other toluene/hexane ratios, a microgel (40:60) and gel-type microporous morphology (100:0) are observed for PM10 and PM20, respectively. The gel-like lamellar structure can be seen in Figure 1(B), and the microgel-

TABLE III
Thermal Stability of the Materials

Polymer	Water (%)	Initial decomposition temperature (°C)	Mass loss (%)	Final decomposition temperature (°C)	Final mass loss (%)
PM10	5	273	6	412	7
PM20	2	283	4	419	19
PM40	5	290	8	426	17

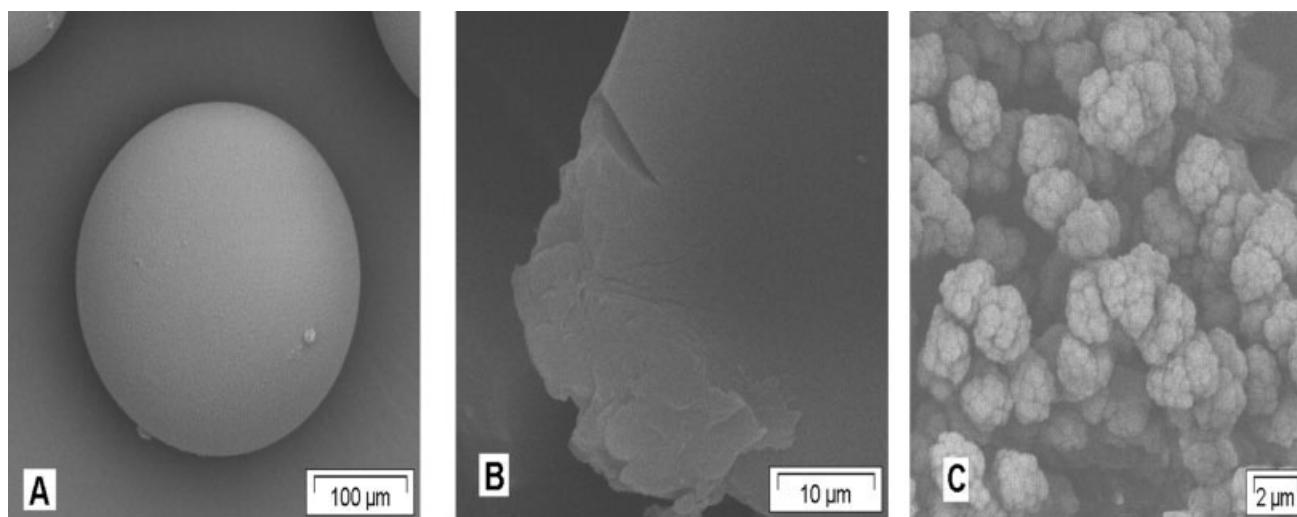


Figure 1 Micrographs of the resin with (A) 40% DVB and 100% toluene (PM40), (B) 20% DVB and 100% toluene (PM20), and (C) 10% DVB and 40% toluene (PM10).

type morphology of the PM10 sample is shown in Figure 1(C). Both are also observed in styrene–DVB resins.²²

The difference of the N_2 adsorption and SEM images can be explained by the structural and morphological differences. In Figure 2, which shows an image of PM40 in which the sphere is cut in half, a number of channels can be observed through the sphere, as happens in a cabbage. This means that it is not a solid sphere. In Figure 3, which shows small structures for PM10, it can be observed that these

structures do not present pores in contrast they present a flakes structure. Therefore, the sphere can adsorb more nitrogen according to the SEM images.

Contact time effect

The chromium retention capability of the pyridine copolymers is presented in Figure 4. The resin (PM10) with the largest nitrogen content (see Table I) is the one for which in a short period the adsorption of metallic ions in a suspension increases

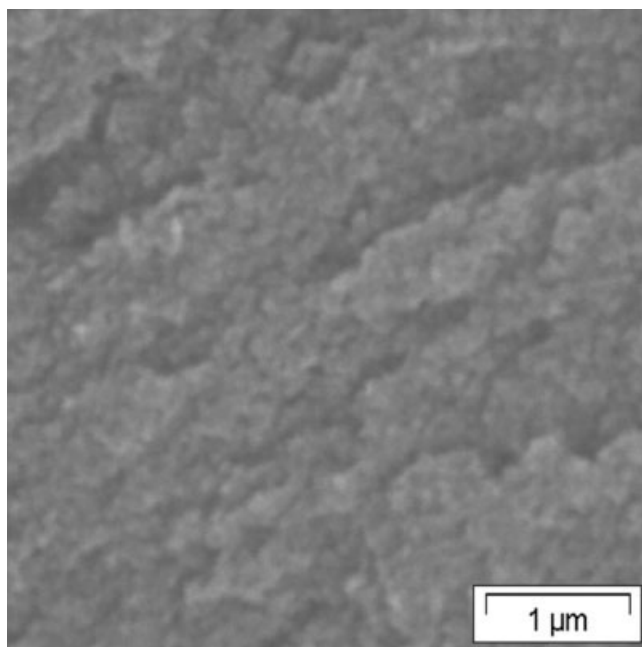


Figure 2 PM40 (20,000 \times). The sphere was cut in half, and the image shows a number of channels through the sphere.

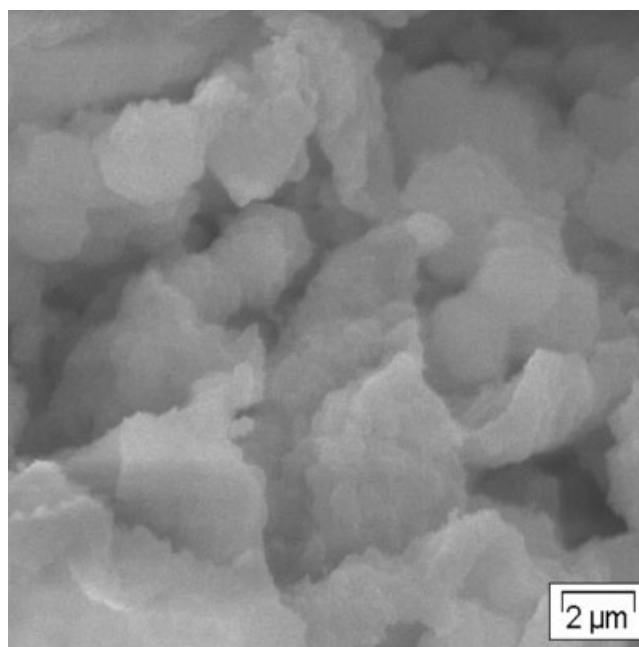


Figure 3 Microgel-type morphology of the PM10 sample (10,000 \times). These structures do not present pores in contrast they present a flakes structure.

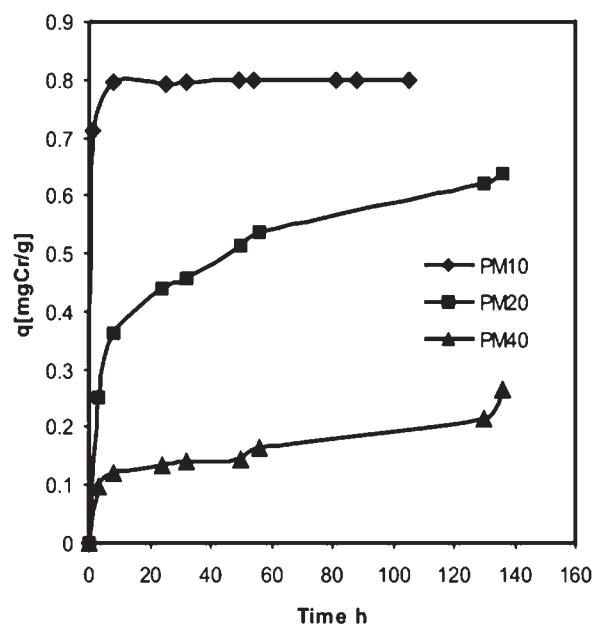


Figure 4 Sorption capability of the macroporous polymers at pH 6.5 and $C_0 = 4$ ppm.

steeply and reaches a sorption capability higher than that of the other resins with a lower concentration of pyridine groups. On the other hand, the polymer with the largest specific surface area but a lower pyridine group concentration (PM40) does not achieve high values of sorption capability. It is quite remarkable that the sorption level of the PM10 resin is not reached comparatively with a very large specific surface area (see Table I); this indicates that the pyridine group content overshadows the effect of the magnitude of the surface area.

During the first 2 h of contact time, the retention capability of polymer PM10 increases steeply and levels off for times longer than 15 h. In the PM20 and PM40 polymers, the sorption capability increases monotonically with time. Because the nitrogen content, that is, the pyridine group content, of the polymers is larger in PM10, this result confirms that the retention capability increases with the number of nitrogen groups in the polymer. On the other hand, the sorption time is modified according to changes in the morphology. PM40 is porous, and it has the largest specific surface area. However, the

sorption rate is restricted by the smaller number of active sites. The polymer PM20 is gel-like and does not present a fast sorption rate, but its retention capability is larger than that of PM40. The PM10 polymer has a wrinkled structure with a faster sorption capability, which indicates that ionic diffusion toward the inner part of the porous structure is fast enough.

To explain the observed behavior of Cr(VI) adsorption at a pH of 6.5, it is necessary to examine the mechanisms involved. At this pH level, the dominant oxyanion species of Cr(VI) are the chromates (CrO_4^{2-}), and because the protonation of the pyridine nitrogen on the poly(4VP) beads is most likely insignificant, electrostatic interaction does not play an important role in the adsorption of Cr(VI) on the sorbent. Therefore, the only possible mechanism is physical adsorption on the sorbent surface. In this respect, it would be interesting to examine the range of low pHs to compare the sorption capability where most of the amine groups located on the sorbent surface are likely to be protonated and possess positive electric charges. The protonated pyridine nitrogen can therefore attract the Cr(VI) species, carrying negative charges in the solution, through the electrostatic interaction mechanism. In this context, the adsorption capability and the adsorption kinetics would increase. This issue is currently being investigated in our laboratory.

The accessibility of the pyridine groups is determined according to the stoichiometry of the reaction with standard 0.3M HCl solutions for titration. The results are shown in Table IV, indicating that the concentration of pyridine groups accessible to PM10 is 74% in a 4 ppm (7.69 mmol) solution and decreases to 52.6% for PM40. The largest value of PM20 (82.4%) is due to the high degree of swelling according to the morphology exhibited by this copolymer. Then, it can be concluded that the adsorption capability is influenced by both the concentration of pyridine groups and the swelling degree.

Adsorption isotherms

This study was carried out with the PM10 sample, that is, the sample with the highest retention capability. Figure 5 shows the Langmuir isotherm results,

TABLE IV
Determination of Active Sites

Sample	Active sites (mmol/g of resin on a stoichiometric basis)	HCl titration of the reactive groups (mmol/g of resin)	Accessibility of the groups (%)
PM10	7.70	5.70	74.0
PM20	6.40	5.28	82.5
PM40	3.92	2.07	52.8

plotting the resin retention capability [q (mg of Cr/g of resin)] versus the residual equilibrium metal concentration (C) according to the following equation:

$$\frac{q}{C} = \frac{q}{K_d} + \frac{q_m}{K_d}$$

where K_d is a constant related to the adsorption energy and q_m is the maximum adsorption capability.

From the linear plot of the sorption capability versus the equilibrium concentration ($R^2 = 0.9922$), it is possible to determine K_d (416 L/mg) and the maximum retention capability (10.33 mg of Cr/g of resin). Arslan et al.,²⁹ using poly(4VP) beads, calculated q_m to be 87 mg of Cr/g of resin at a pH of 3. The difference is that at a low pH, the pyridine groups are protonated and have better adsorption capacity. This result agrees with those of other authors.^{19,30} In the resins studied here, the physical adsorption mechanism is shown because the pH is 6.5, the pyridine group is not protonated, and the chromium ion is only adsorbed.

FTIR spectra

The IR spectrum of PM10 (the copolymer with 10% DVB and 90% 4VP) is presented in Figure 6. Adsorption bands from 1415 to 1597 cm^{-1} , assigned to aromatic rings, correspond to the C=C and C=N vibrations, whereas the band at 3023 cm^{-1} corresponds to the C=H group vibration in the aromatic ring. Adsorption bands at 2926 and 1475–1450 cm^{-1} are assigned to the CH₂ of the ethyl group or aliphatic chain. The vibration at 820 cm^{-1} is characteristic of disubstituted aromatic rings. The peak at 943 cm^{-1} in the spectrum is due to the resonance peak of the

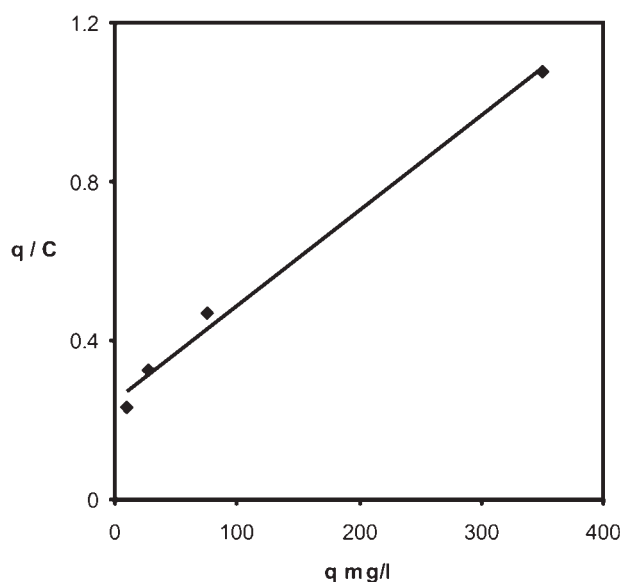


Figure 5 Langmuir isotherm for PM10 at pH 6.5.

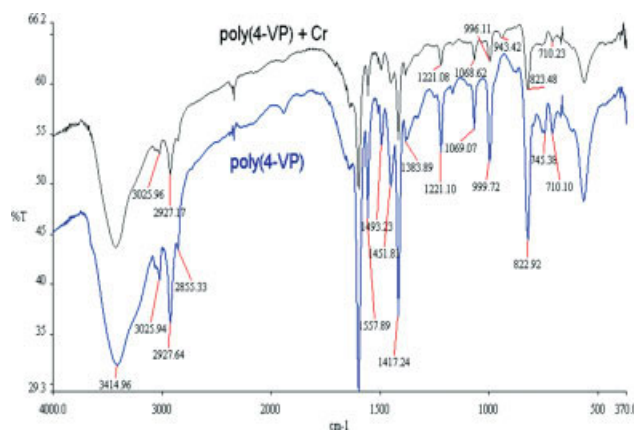


Figure 6 FTIR spectra of the resin and Cr(VI) adsorbed onto PM10. [Color figure can be viewed in the online issue, which is available at www.interscience.wiley.com.]

Cr—O and Cr=O bonds from the Cr(VI) species and suggests that Cr(VI) was adsorbed onto the surface and the nitrogen atoms on poly(4VP) of the copolymer were involved in the adsorption. In contrast, Arslan et al.²⁹ also described this last peak, but they observed it at 934 cm^{-1} . Finally, the band at 3434 cm^{-1} corresponds to the —OH bond due to the presence of water.

CONCLUSIONS

Copolymers were synthesized in this work under several reaction conditions with changes in the DVB content, which induced changes in the morphology and specific surface area, producing efficient resins for Cr⁺⁶ removal at pH 6.5. The resultant morphologies were affected by different porogen agents. A relevant conclusion of this work is that the most important factors in metal sorption are the concentration of pyridine groups and swelling capability. Morphology is also an important factor that influences the sorption rate.

References

- Lee, M.-Y.; Hong, K.-J.; Yoshitsune, S.-Y.; Kajuchi, T. *J Appl Polym Sci* 2005, 96, 44.
- Lasko, C. L.; Adams, K. H.; Benedet, E. M.; West, P. A. *J Appl Polym Sci* 2004, 93, 2808.
- Humphries, A. C.; Macaskie, L. *J Chem Technol Biotechnol* 2005, 80, 1378.
- Bringas, E.; Fresnedo, M.; Ortiz, I. *J Chem Technol Biotechnol* 2006, 81, 1829.
- Rivero, M. J.; Primo, O.; Ortiz, I. *J Chem Technol Biotechnol* 2004, 79, 822.
- Forstner, U.; Wittmann, G. T. W. *Metal Pollution in the Aquatic Environment*; Springer-Verlag: Berlin, 1983.
- Edwards, J. D. *Industrial Wastewater Treatment*; CRC/Lewis: Boca Raton, FL, 1995.
- Salazar, E.; Ortiz, M. I.; Urriaga, A. M.; Irabien, J. A. *Ind Eng Chem Res* 1992, 31, 1523.

9. Vincent, T.; Guibal, E. *Ind Eng Chem Res* 2001, 40, 1406.
10. Sengupta, A. K. In *Ion Exchange Technology—Advances in Pollution Control*; Sengupta, A. K., Ed.; Technomic: Lancaster, PA, 1995; p 115.
11. Sengupta, A. K.; Clifford, D. *Ind Eng Chem Fundam* 1986, 25, 249.
12. Gang, D.; Hu, W.; Banerji, S. H.; Clevenger, T. E. *Ind Eng Chem Res* 2001, 40, 1200.
13. Rabelo, D.; Silva, V. J.; Alcantara, E. F. C.; Faria, L. C.; Martins, G. A. V.; Garg, V. K.; Oliveira, A. C.; Morais, P. C. *J Appl Polym Sci* 2003, 89, 3905.
14. Gutanu, B. L.; Maturana, H. A.; Luna, M. *J Appl Polym Sci* 1999, 74, 1557.
15. Sun, C.; Qua, R.; Wang, Q.; Ji, C.; Wang, C.; Xu, Q.; Fang, X.; Cheng, G. *J Appl Polym Sci* 2006, 100, 4581.
16. Auki, S. K.; Neufeld, R. D. *J Chem Technol Biotechnol* 1997, 70, 3.
17. Wang, C. C.; Chen, C. Y.; Chang, C. Y. *J Appl Polym Sci* 2002, 84, 1353.
18. Lutfor, M. R.; Sidik, S.; Wan Yunus, W. M. Z.; Rahman, M. Z. A.; Mansor, A.; Haron, M. J. *J Appl Polym Sci* 2001, 79, 1256.
19. Rivas, B. L.; Maturana, H. A.; Luna, M. *J Appl Polym Sci* 1999, 74, 1557.
20. Sugii, A.; Ogawa, N.; Iinuma, Y.; Yamamura, H. *Talanta* 1981, 28, 551.
21. Low, K. S.; Lee, C.; Low, C. *J Appl Polym Sci* 2001, 82, 2128.
22. Sherrington, D. C. *Chem Commun* 1998, 2275.
23. Kari, A. N.; Hagen, S.; Berge, A. *J Appl Polym Sci* 1999, 37, 3973.
24. Albright, R. L. *React Polym* 1986, 4, 155.
25. Okay, O. *Prog Polym Sci* 2000, 25, 711.
26. McCurdie, M. P.; Belfiore, L. A. *Polymer* 1999, 40, 2889.
27. Sugii, A.; Ogawa, N.; Iinuma, Y.; Yamamura, H. *Talanta* 1981, 28, 551.
28. Neagu, V.; Untea, I.; Tudorache, E.; Orbeci, C. *J Appl Polym Sci* 2004, 93, 1957.
29. Arslan, M.; Yigitoglu, M.; Soysal, A. *J Appl Polym Sci* 2006, 101, 2865.
30. Horak, D.; Benes, M. J.; Gumargalieva, K. *J Appl Polym Sci* 2001, 80, 913.
31. Herrmann, M. S. *J Chem Educ* 1994, 71, 323.